

PRACTICAL SUPERCONDUCTOR DEVELOPMENT  
FOR ELECTRICAL POWER APPLICATIONS

ARGONNE NATIONAL LABORATORY

QUARTERLY REPORT FOR THE PERIOD ENDING JUNE 30, 2000

RECEIVED  
SEP 07 2000  
O.S.T.I.

This is a multiyear experimental research program focused on improving relevant material properties of high- $T_c$  superconductors (HTSs) and on development of fabrication methods that can be transferred to industry for production of commercial conductors. The development of teaming relationships through agreements with industrial partners is a key element of the Argonne (ANL) program.

**Technical Highlights**

Recent results are presented on  $\text{YBa}_2\text{Cu}_3\text{O}_x$  (Y-123) coated conductors, including microstructural studies and deposition of yttria-stabilized zirconia (YSZ) deposited by ion-beam-assisted deposition (IBAD); fundamental studies of grain-boundary pinning in Y-123; and Ag-sheathed  $\text{Bi}_2\text{Sr}_2\text{CaCu}_2\text{O}_x$  (Bi-2212) and  $(\text{Bi,Pb})_2\text{Sr}_2\text{Ca}_2\text{Cu}_3\text{O}_x$  (Bi-2223) tapes.

Microstructural Characterization of Coated Conductors

To improve the critical current densities ( $J_c$ s) of Y-123 thin films on flexible metallic substrates, films have been deposited on textured buffer layers. Electron microscopy has been used to investigate the microstructure, grain size, thickness and crystal orientation of these buffer layers prior to Y-123 deposition, with the goal of optimizing texture. Y-123 films deposited on the optimized layers were also examined by electron microscopy.

Scanning electron microscopy (SEM) was performed in a Hitachi S4700 field-emission-gun microscope. Samples were prepared by either fracturing the specimen and examining as-is or mechanical polishing. Transmission electron microscopy (TEM) was carried out in a Philips CM30. Plan-view TEM specimens were prepared by mechanical grinding, dimpling, and ion-milling from the undeposited side of the sample. Cross-sectional TEM specimens were prepared by gluing two pieces of deposited material face-to-face, followed by mechanical grinding, dimpling, and ion-milling.

Biaxially textured yttria YSZ buffer layers were deposited on randomly oriented Hastelloy C and 304 stainless steel substrates by IBA. Deposition was at room temperature with varying ion-to-atom arrival ratios (r-values).

## **DISCLAIMER**

**This report was prepared as an account of work sponsored by an agency of the United States Government. Neither the United States Government nor any agency thereof, nor any of their employees, make any warranty, express or implied, or assumes any legal liability or responsibility for the accuracy, completeness, or usefulness of any information, apparatus, product, or process disclosed, or represents that its use would not infringe privately owned rights. Reference herein to any specific commercial product, process, or service by trade name, trademark, manufacturer, or otherwise does not necessarily constitute or imply its endorsement, recommendation, or favoring by the United States Government or any agency thereof. The views and opinions of authors expressed herein do not necessarily state or reflect those of the United States Government or any agency thereof.**

## **DISCLAIMER**

**Portions of this document may be illegible in electronic image products. Images are produced from the best available original document.**

A cross-sectional TEM image of a YSZ film with an  $r$ -value of 2.8, grown on Hastelloy C, is shown in Fig. 1. It can be seen that the microstructure of the YSZ film consists of columnar grains that increase in width as the film becomes thicker. Selected area diffraction (SAD) patterns were obtained at four different points in the film, shown in the figure as points A, B, C, and D. The pattern at the bottom of the film (A) is indicative of a randomly oriented polycrystalline film and gradually changes as the film becomes thicker, while the pattern at the top (D) demonstrates preferred texture. These results indicate that grains that are aligned favorably with the ion source dominate the structure as the film grows.

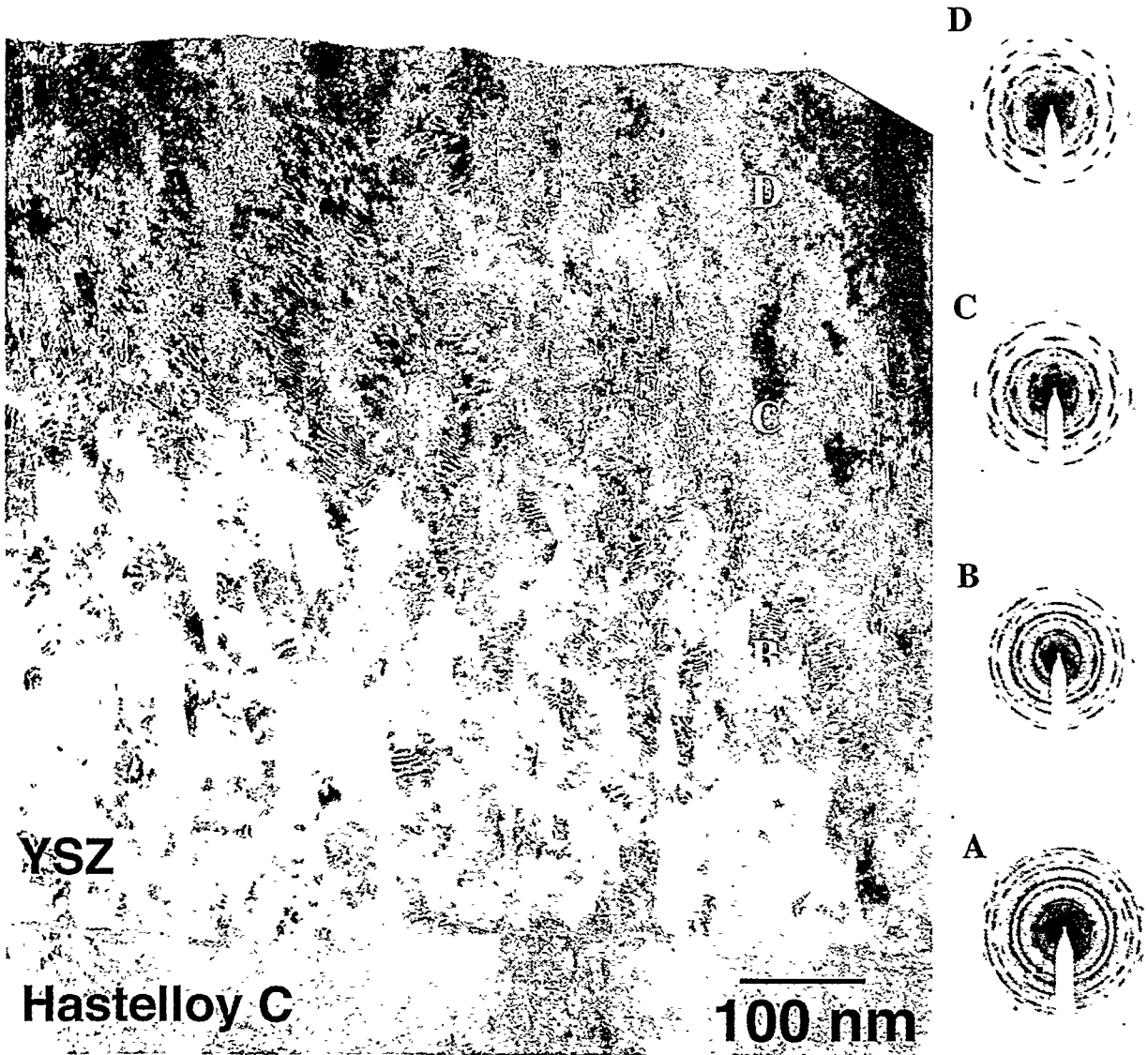


Fig. 1. Cross-sectional TEM photomicrograph of IBAD YSZ layer on Hastelloy C substrate and electron diffraction patterns from various regions.

Y-123 has been deposited on YSZ buffer layers, with good results. Figure 2 is an SEM image of YSZ on which a  $\text{CeO}_2$  cap layer was deposited, followed by Y-123. The image was acquired with backscattered electrons in order to observe differences in elemental composition. Figure 3 is a cross-sectional TEM image of the same sample; it shows that crystalline Y-123 was deposited.

Progress is also being made in the growth of MgO buffer layers made by inclined substrate deposition (ISD). Biaxially textured MgO films were deposited on silicon substrates by inclined substrate deposition. Figure 4 is a plan-view TEM image of an MgO film deposited at a substrate inclination angle of  $55^\circ$ . Two important features can be seen: the cubic morphology of the grains and the large angular gaps between rows of crystals. These features are due to the preferential growth of the (200) equilibrium crystal habit of MgO and shadowing by columnar grains.

#### Deposition of Buffer Layers for Coated Conductors

Previous work has firmly established that the degree of texture development in YSZ films produced by IBAD is primarily dependent on the ratio of ions to atoms, i.e., r-value, arriving at the substrate surface during processing. The r-value can be changed by varying the ion beam current density ( $I_b$ ) and deposition rate. In the present work, film development was studied primarily by evaluating the degree of



Fig. 2. SEM photomicrograph of Y-123 coated conductor, with YSZ deposited by IBAD.

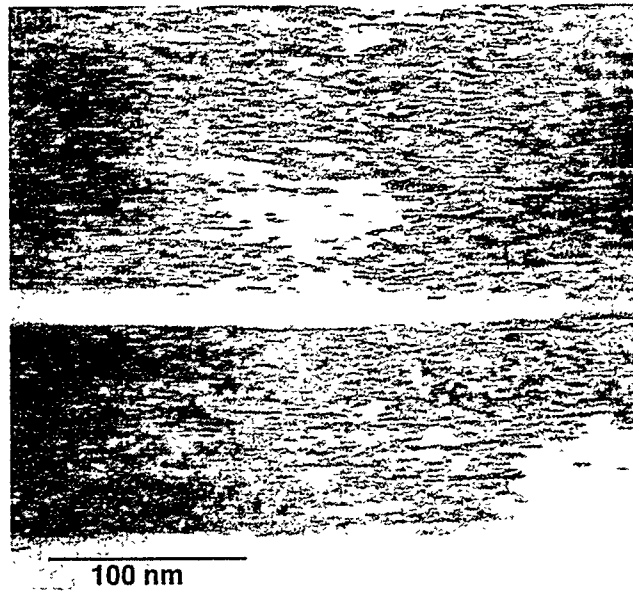


Fig. 3. Cross-sectional TEM photomicrograph of Y-123 layer on CeO<sub>2</sub>/YSZ/Hastelloy C substrate.

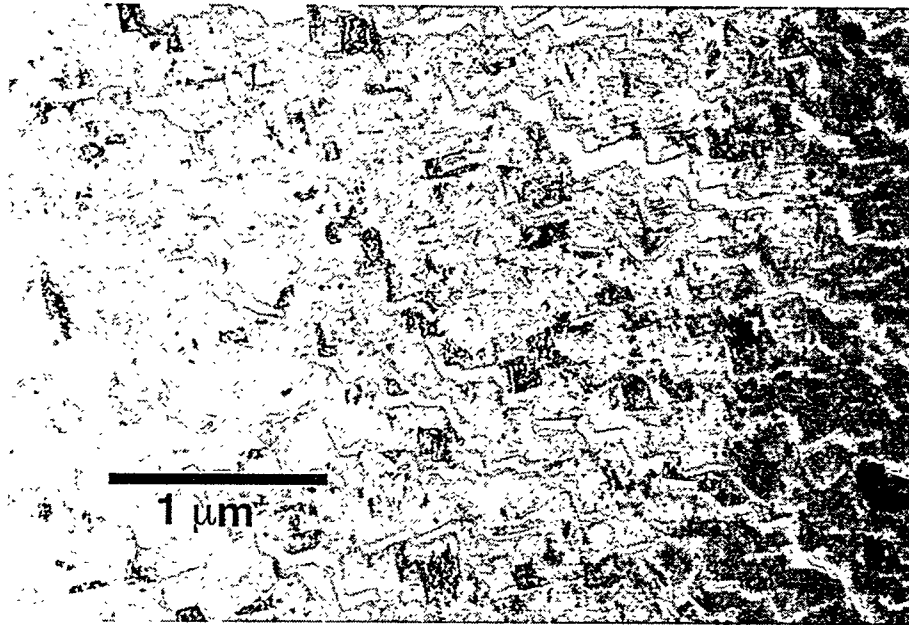


Fig. 4. Plan-view TEM photomicrograph of ISD MgO layer.

texture versus film thickness for various  $r$ -values at a constant ion-bombardment angle of  $55^\circ$  from an 8-cm ion source, with an ion-beam energy of 300 eV. The goal was to identify the optimal  $r$ -value for YSZ deposition.

As-received polycrystalline Hastelloy C was used as the substrate; 100- $\mu\text{m}$ -thick Hastelloy C sheet was sheared into 1  $\text{cm}^2$  coupons and polished with diamond paste to a finish of 0.1  $\mu\text{m}$ . The substrates were ultrasonically cleaned in acetone,

and further cleaned by swabbing the surface with ethanol. Partially shielded Si substrates were placed adjacent to the Hastelloy C substrates so that film thicknesses could be determined accurately. The base pressure of the deposition chamber before ion bombardment was  $10^{-7}$  torr, which rose to an operating pressure of  $9 \times 10^{-5}$  torr with initiation of the Ar and O<sub>2</sub> gas flow into the ion source. The O<sub>2</sub> flow rate was set to 10% of that of Ar.

The r-value was varied by changing  $I_b$  and measuring the corresponding ion fluence at the substrate surface by the Faraday cup. An accurate ion fluence, varied between 3 and 7  $\mu\text{A}$ , was ensured by proper positioning of a Faraday cup for each deposition. After generation of a steady ion bombardment, evaporation of the YSZ began. While focused onto the evaporation hearth, the power to the electron beam was initially held low to condition the YSZ. Following conditioning, the power was steadily increased manually to the desired deposition rate displayed on the crystal quartz rate monitor. After constant deposition rate and ion bombardment were ensured, IBAD was initiated. The deposition rate was varied from 0.4 to 2.0  $\text{\AA}/\text{s}$ , and all depositions were made to a thickness of 0.8  $\mu\text{m}$ .

Biaxial texture was characterized with a Scintag four-circle X-ray diffractometer (CuK $\alpha$  radiation). Standard  $2\theta$  scans were used to determine any preferred crystalline orientation. The degree of out-of plane texture was determined by the full-width-at-half-maximum (FWHM) of  $\Omega$  scans of the YSZ (200) reflection. In-plane texture was measured by the FWHM of  $\phi$  scans of the YSZ (111) reflection. (111) pole figures were generated to map out extents of biaxial texture.

X-ray analysis was performed on the IBAD YSZ/Hastelloy C substrates. YSZ films deposited without ion assistance ( $r = 0$ ) were essentially amorphous. Increasing r-values up to 1 induced a gradual increase in (111) preferred growth. The ions presumably provided sufficient surface mobility for the adatoms of YSZ to preferentially grow with a  $\langle 111 \rangle$  direction normal to the surface. Studies on preferred growth of IBAD YSZ as a function of substrate temperature have noted formation of (111) at lower r-values and higher temperatures. Without the assisting ion beam or at low r-values, formation of (111) surfaces is most stable, whereas at larger r-values, the ion beam limits the mobility of adatoms and promotes growth of (200) surfaces.

Films produced at an r-value of 1.6 showed both (111) to (200) orientations; r-values above 1.6 produced (200) preferential growth. At large r-values, the intensity dropped off due to the decreased film thickness because of sputtering and concomitant X-ray penetration into the substrate. Figure 5 illustrates the effect of r-value on preferential growth of IBAD YSZ. It can be expected that the (200) orientation remains up to a critical r-value,  $r_c$ , at which more material is sputtered away than deposited.

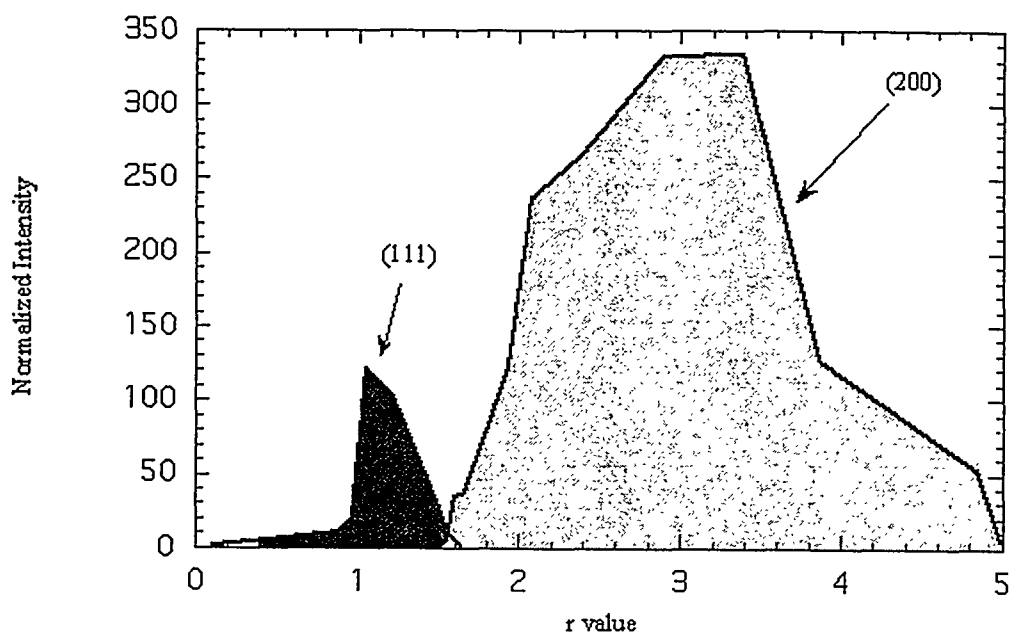


Fig. 5.  $\theta$ - $2\theta$  relative intensity as a function of  $r$ -value, illustrating zones of preferred orientation.

The degree of  $c$ -axis, out-of-plane texture was determined by  $\Omega$  scans performed on the (200) reflection. At  $r$ -values  $> 2$ , all films with (200) preferred texture exhibited good  $c$ -axis alignment, with full-width-at-half-maximum (FWHM) values to  $\approx 5^\circ$ . Previous studies on various substrate materials have shown that out-of-plane texture forms readily and is mostly dependent on the surface roughness of the substrate. This is expected due to growth rate anisotropy and the tendency toward columnar-growth structures in YSZ.

To quantify the degree of in-plane texture,  $\phi$  scans of the YSZ (111) reflection were performed. Figure 6 is a  $\phi$  scan for a film with an  $r$ -value of 2.32; four symmetric (111) peaks are observed. FWHM determinations of a Gaussian curve fits were used to characterize the degree of biaxial texture.

The in-plane texture of IBAD YSZ was studied for  $r$ -values of 1.4 to 6. Figure 7, a graph of FWHM as a function of  $r$ -value, reveals a steady improvement in texture with increasing  $r$ -value up to  $r \approx 3$ . Thereafter, the increase of FWHM saturated with  $r$ -values of  $\approx 6$ .

As the number of ions that hit the surface increases, more of them satisfy the criteria for ion channeling and contribute to an increase in anisotropic ion etching and overgrowth of crystallites having orientations other than those of the biaxially aligned YSZ (200) grains. Thus, increasing the ion flux allows the (200)

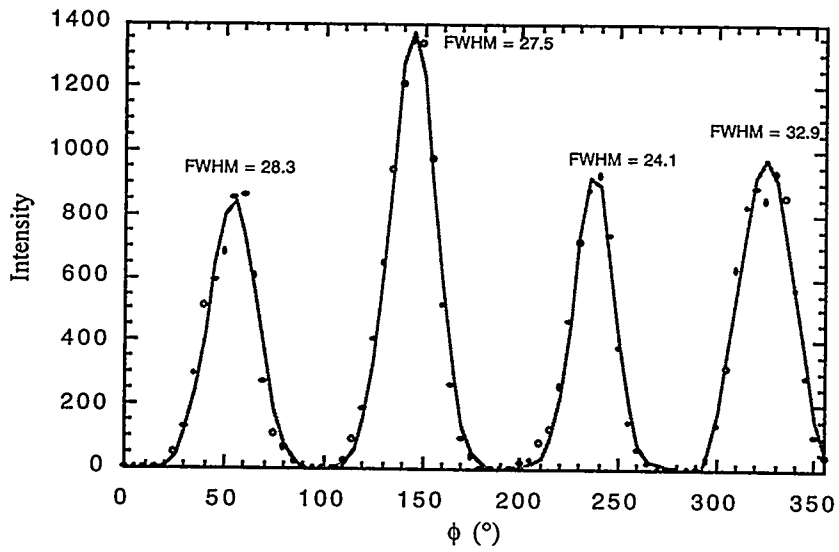


Fig. 6.  $\phi$  scan of IBAD YSZ film produced with r-value of 2.32, indicating in-plane biaxial texture.

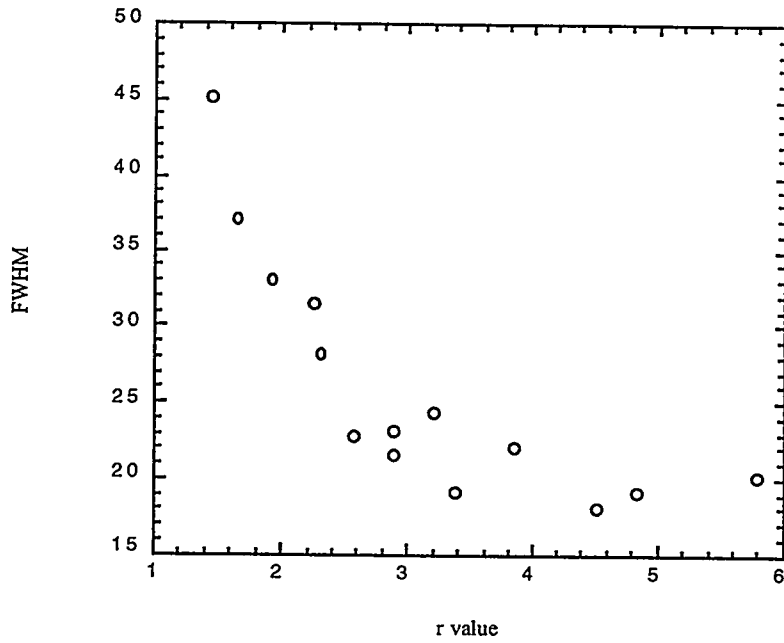


Fig. 7. Effects of r-value on in-plane texture of IBAD YSZ films.

faster-growing grains to grow and further align themselves with respect to the ion beam. It has been shown that the degree of in-plane texture increases asymptotically to the critical value  $r_c$ , where more material is sputtered away than deposited. Therefore, the degree of in-plane texture should also increase to a critical value. This effect is evident in Fig. 7.

The 8-cm ion source used in this work is capable of achieving an overall FWHM of  $\approx 17^\circ$ . However, glancing-angle X-ray studies have shown that surface textures are substantially sharper than those of the bulk, typically  $\approx 9^\circ$  less in the FWHM. This implies that an IBAD YSZ film produced with an in-plane texture of  $17^\circ$  would correspond to a surface FWHM of  $8^\circ$  and would therefore yield Y-123 films with  $J_{cs} > 10^6$  A/cm<sup>2</sup> at 77 K.

Film thicknesses on the partially shielded Si control samples are plotted as a function of r-value in Fig. 8. The decrease in thickness for an increasing r-value approximately follows a linear trend. From a linear fit, a calculated thickness,  $z_t$ , was used to determine the loss in thickness,  $\Delta z$ , due to ion etching. Assuming an equal packing density for a film deposited without ion assistance, the number of atoms sputtered away,  $n_a$ , could be calculated for each deposition by the thickness loss  $\Delta z = 1.64 - z_t$ . The ion number density  $n_i$  was also calculated.

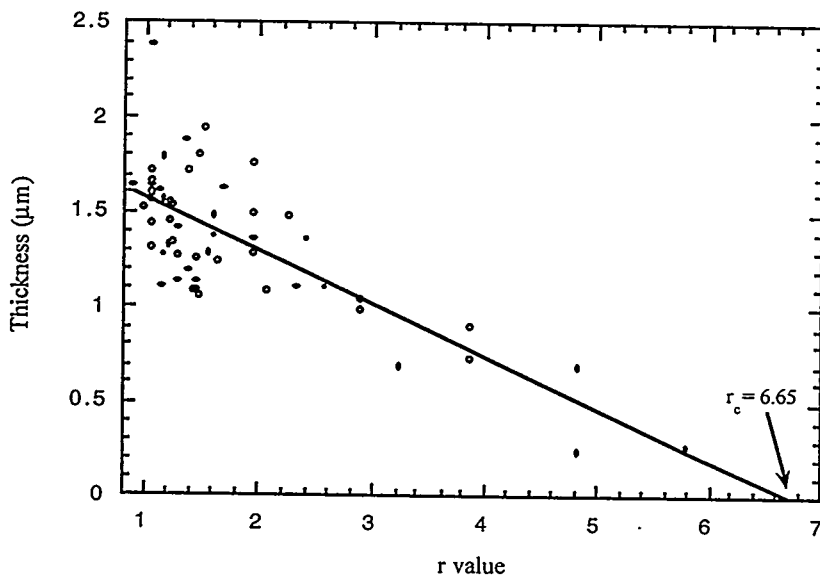


Fig. 8. Film thickness as function of r-value.

The sputter yield,  $n_a/n_i$ , for a 300-eV ion beam and bombardment angle of  $55^\circ$  as a function of r-value is shown in Fig. 9. The YSZ sputter yield was found to increase rapidly with r-value, presumably because of the increased number of ions hitting the surface and dislodging YSZ surface atoms. The sputter yield rate of increase tapered off as the r-value approached the critical value  $r_c$ .

### Y-123 Grain Boundaries

In collaboration with R. Feenstra and D.K. Christen of the Solid State Division at Oak Ridge National Laboratory, we recently obtained critical current data on bicrystal grain boundaries (GBs). The data exhibited a peak in the GB critical current,  $I_{cb}(H)$ , and an unusual inverse hysteresis. The results give considerable support to a new mechanism for an enhanced GB critical current, which was recently proposed by Gurevich and Cooley of the University of Wisconsin. The enhanced GB critical current arises from pinned Abrikosov vortices in the banks of a GB, which present a static, quasiperiodic pinning potential to pin GB vortices. Model calculations predict a peak in  $J_c(H)$ . Further support for the Gurevich-Cooley model arises from the history dependence of  $I_{cb}(H)$  and the field profiles found in these bulk materials. We have measured  $I_{cb}(H)$  of the GB after either

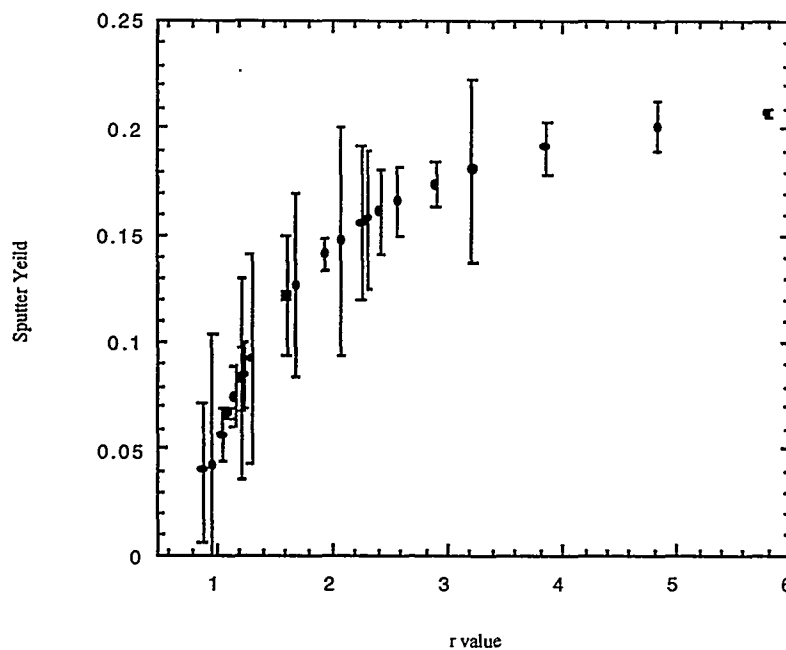


Fig. 9. Sputter yield of YSZ surface versus r-value for  $55^\circ$ , 300 eV  $\text{Ar}^+$  ion beam.

(1) field cooling (FC) the sample in an applied field,  $H$ , to a temperature,  $T$ , from *above* the transition temperature,  $T_c$ ; or (2) increasing  $H$  after zero-field cooling (ZFC) to  $T$  (Fig. 10). In low fields, the GBs exhibit a higher  $I_{cb}$  for FC, which is just opposite to the usual hysteresis for the grains of bulk materials (in which the greater internal fields associated with FC decrease the pinning and thus  $I_{cg}$ ). However, this is exactly the expectation of the Gurevich-Cooley model for GBs, because FC provides a higher Abrikosov vortex density in the banks that can more strongly pin GB vortices.

Magnetization data on the same sample are consistent with features of the  $I_{cb}$  hysteresis interpreted in this framework, including the irreversibility field, above which the internal flux profiles are nearly the same for FC and ZFC. Above the irreversibility field, a necessary expectation of the model is that the GB transport should be indistinguishable between FC and ZFC, and our data confirm this.

### Bi-2212 Wire Development

Ag/Al-sheathed multifilament Bi-2212 wires have been heat-treated at various peak temperatures from 880 to 900°C. Critical currents of the samples were measured at 77 K. Figure 11 shows the dependence of peak temperature on critical current of the conductors, which were postannealed at 450°C in Ar. It has been shown that this annealing increases the  $I_c$  of the samples at 77 K, but reduces the  $I_c$  of the samples at 4.2 K. In this study, the highest  $I_c$  was obtained with heating at 891°C. This indicates that significant melting is necessary to achieve high  $J_c$ .

A further study was made of the cooling rate after the melting stage, with the peak temperature fixed at 891°C. The cooling rates were varied from 3°C/h to 15°C/h. A cooling rate of  $\approx 7^\circ\text{C}/\text{h}$  yielded the highest  $I_c$  at 77 K.

As reported in the December 1999 Quarterly Report, we have found a relationship between  $I_c$  at 77 K and  $I_c$  at 4 K.  $I_c$  measurements were also conducted at 4.2 K in applied magnetic fields (Fig. 12). For these Bi-2212 wires, there was no post-annealing in Ar. The sample in Fig. 12 exhibited an  $I_c$  of 0.51 A at 77 K and 200 A at 4.2 K in self-field. At 4.2 K and 6 T, the sample maintained 36% of its zero-field  $I_c$ . Transport  $J_c$  at 4.2 K was 167 kA/cm<sup>2</sup>. The highest  $J_c$  we can expect from our best wires is estimated to be  $\approx 220$  kA/cm<sup>2</sup>.

To reduce AC losses of the Bi-2212 wires, insulating layers are being applied to reduce the coupling loss. SrZrO<sub>3</sub>, BaZrO<sub>3</sub>, and ZrO<sub>2</sub> have been used as the insulating materials. In one method, the insulating materials were packed into the Ag-alloy tube along with Bi-2212 filaments. In another method, the insulating materials were dip-coated before mechanical working. The latter method ensured that the individual filaments were isolated from each other. The conductor was preheat-treated to burn out the organics before drawing.

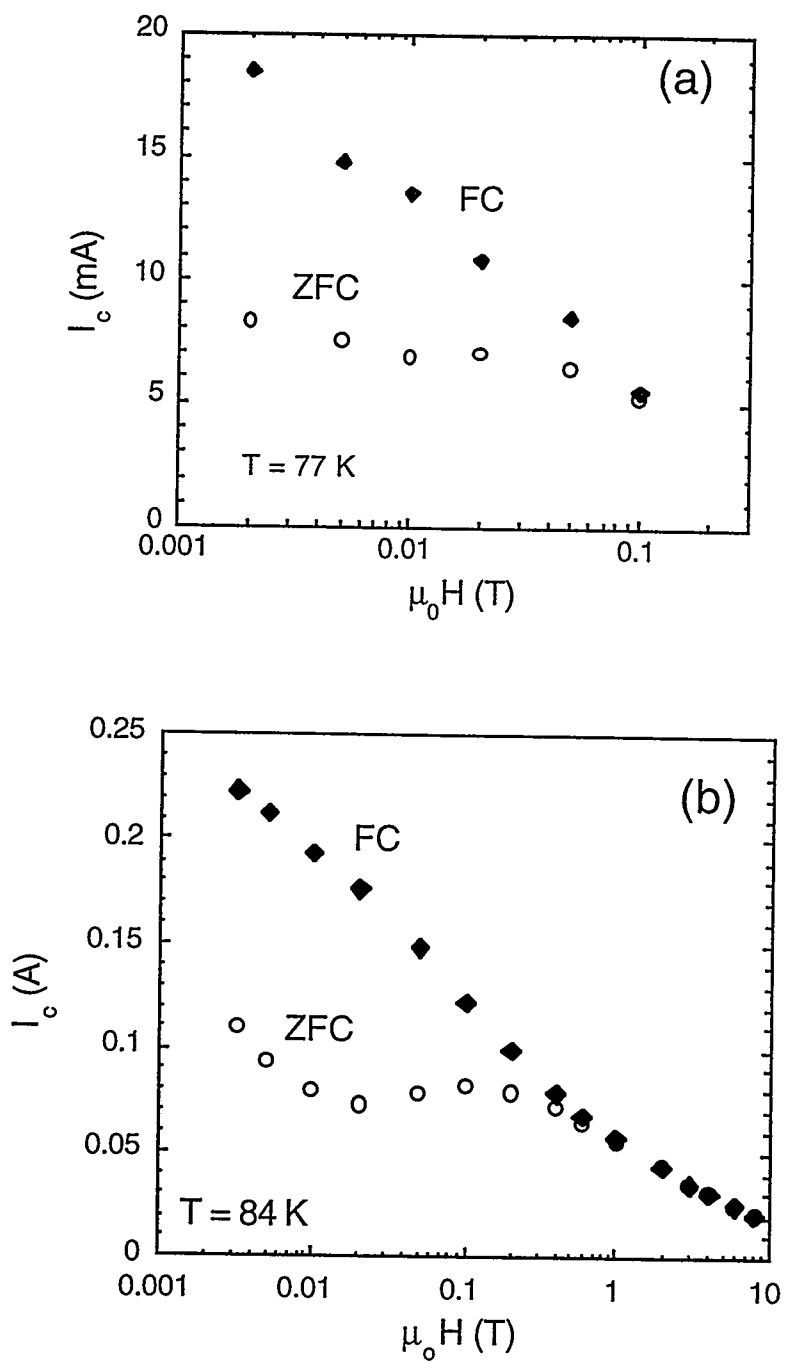


Fig. 10.  $I_{cb}$  data for FC and ZFC for GBs in Y-123; data obtained from (a)  $11^\circ$  [001] tilt GB in coated conductor and (b)  $90^\circ$  [100] tilt GB in bulk sample.

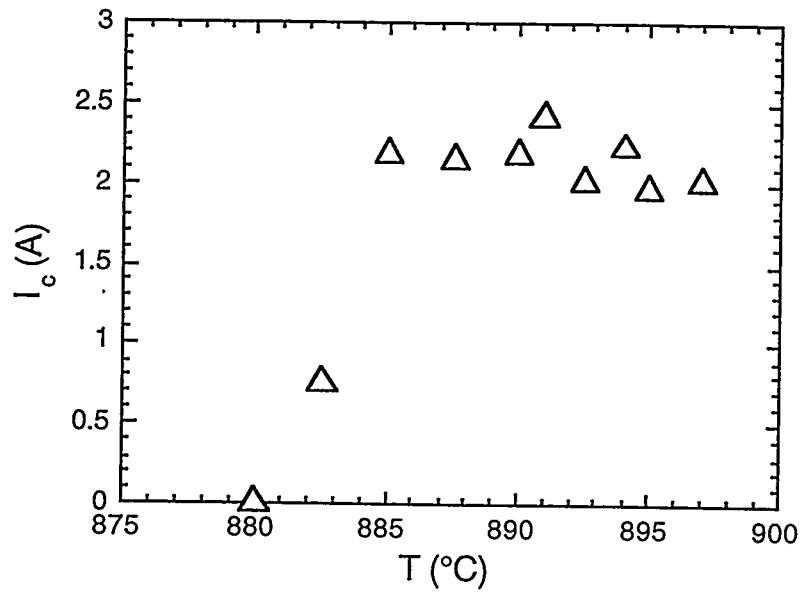


Fig. 11. Dependence of  $I_c$  of Bi-2212 wires on peak temperature during heat treatment.

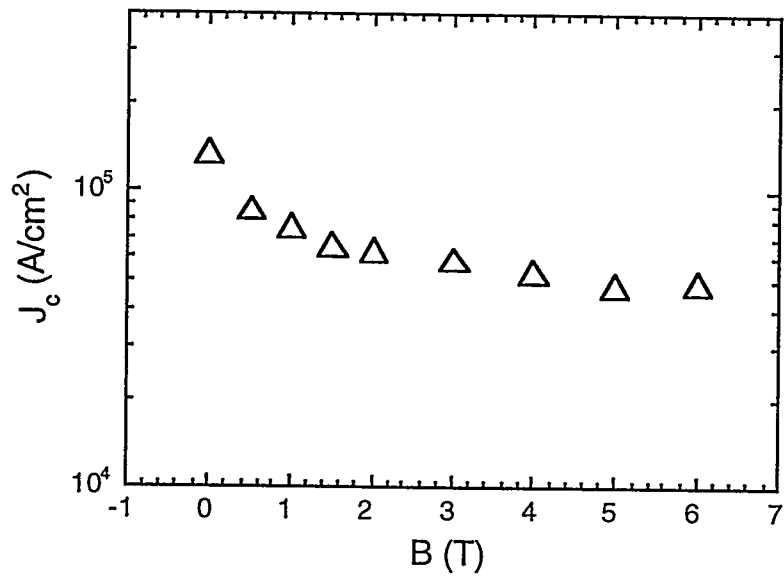


Fig. 12.  $J_c$  at 4.2 K vs. applied magnetic field for round multifilament Bi-2212 wire.

The insulating layers obtained were found to be uniform and dense according to SEM observations. They have been shown to be chemically stable at high temperatures.

### Hardened Sheaths for Bi-2223 and Bi-2212 Conductors

Internal oxidation of Ag-Mg alloys increases yield strength substantially. Increased yield strength is required for the sheaths of Bi-2223 and Bi-2212 tapes and wires. We have continued our studies of the phenomenon and have developed a processing schedule that imparts a uniform yield strength of 200 MPa to Ag/1.2 at.% Mg. The key to this process is formation of oxygen-rich Mg-O clusters within the Ag. The superstoichiometry of O with respect to Mg in these clusters decreases as they become larger. A schematic diagram of the smallest Mg-O cluster is shown in Fig. 13. Actual clusters within a specimen that was heated in 8% O<sub>2</sub> for 50 h are shown in Fig. 14.

The Mg-O clusters are stable with prolonged heating at temperatures to 825°C. Although larger clusters have a tendency to form preferentially along grain boundaries (Fig. 15), most of the smaller clusters remain within the grains, and thus the increases in yield strength over that of pure Ag are substantial.

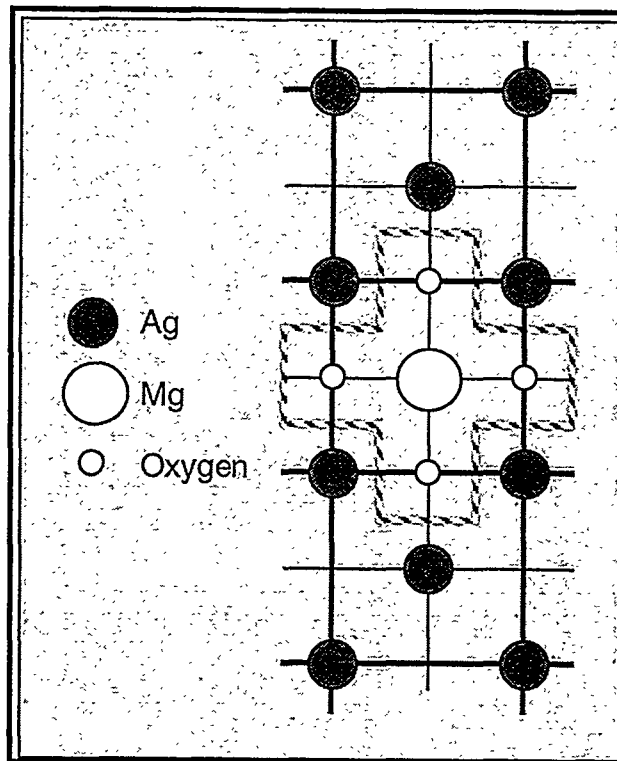


Fig. 13. Two-dimensional representation of Mg-O cluster in Ag lattice; O/Mg = 4.

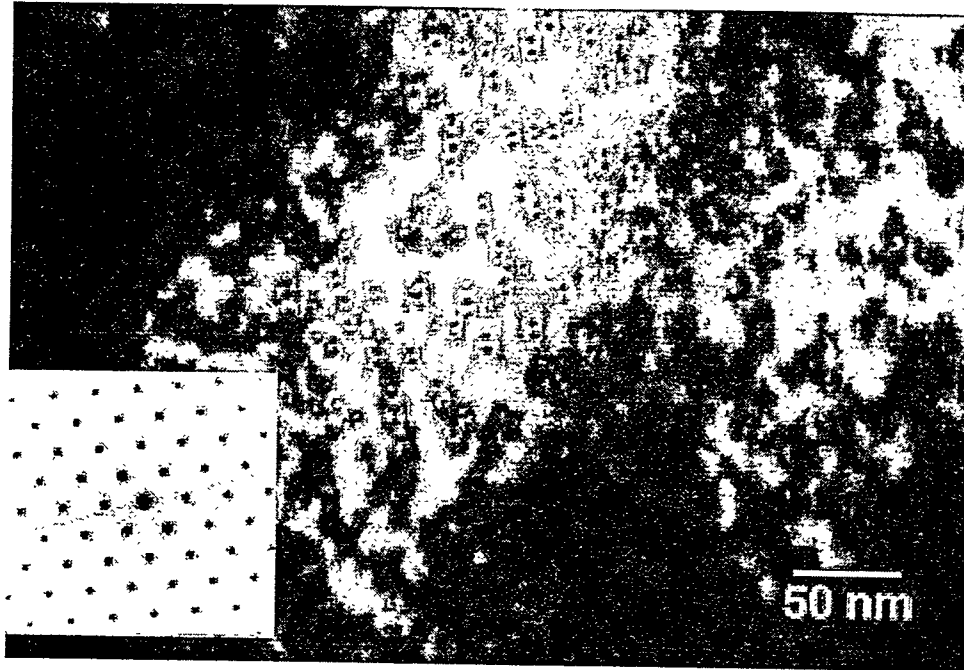


Fig. 14. Transmission electron microscopy photomicrograph of Mg-O clusters in alloy heated at 850°C for 50 h.

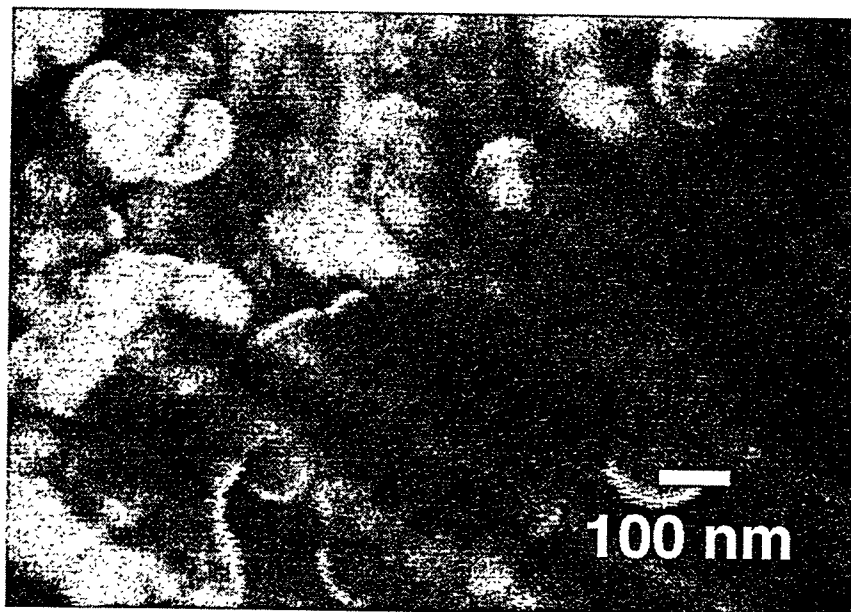


Fig. 15. Scanning electron microscopy photomicrograph of large Mg-O clusters near grain boundary in alloy heated at 850°C for 50 h.

## Interactions

Several members of the program attended the Annual Meeting of the American Ceramic Society in St. Louis, on April 1–3. Balu Balachandran, Bart Prorok, and Tom Truchan presented talks. Beihai Ma, J. P. Singh, and Young Jee participated in many discussions.

On April 6, Tom Truchan successfully defended his M.S. thesis at the Illinois Institute of Technology, thereby completing the requirements for his degree. Tom's research with Ken Goretta focused on optimization of IBAD processing for coated conductors.

Balu Balachandran presented ANL's tasks in FY 2000 and plans for FY 2001 at the FWP Review in Washington, DC, on May 4.

On May 8, Balu Balachandran reviewed the MicroCoating Technologies (MCT) Phase I results and future plans in Atlanta.

Srinath Athur, who worked as an ANL Lab-Grad student, successfully defended his Ph.D. thesis research on kinetics of melt-processing of the RE-123 system at the University of Houston on May 18.

Balu Balachandran was invited to participate in the European Topical Workshop on Coated Conductors in Göttingen, Germany, on May 26-27.

On May 30, Mr. Seung Woo Lee (Ministry of Commerce, Industries & Energy, Republic of Korea), Dr. Sang-Joon Kim (Korea Electric Power Research Institute), Dr. Tae-Hyun Sung (Korea Electric Power Research Institute), and Dr. Sang-Soo Oh (Korea Industrial Development Institute) visited ANL to discuss our superconductor program and, in particular, the flywheel project.

Balu Balachandran attended the Intermagnetics General Corporation—SuperPower HTS facility dedication and partner appreciation ceremony in Schenectady, NY, on June 7.

Mike Chudzik successfully defended his Ph.D. thesis at Northwestern University on June 9. Mike's work with Balu Balachandran focused on development of textured buffer layers and Y-123 films for coated conductors.

Balu Balachandran was invited to participate at the ICMC 2000—Application of Superconductors Conference in Rio de Janeiro, Brazil, June 12-13.

Prof. Mike Lanagan of the Pennsylvania State University visited ANL on June 12. Several topics related to superconductor fabrication and characterization were discussed.

On June 13, Balu Balachandran attended the Detroit Edison cable project quarterly review at DOE in Washington, DC.

Balu Balachandran presented a talk on high temperature superconductors at the Energy Frontiers International meeting in Ottawa, Canada, June 19-20, 2000.

On June 22, Balu Balachandran reviewed ANL's program and plans with the program manager at DOE in Washington, DC.

Balu Balachandran attended the ANL-Los Alamos National Laboratory-IGC CRADA technical review meeting at Los Alamos on June 27.

### List of Publications

#### Published or presented:

B. Venkateshwaran, R. Guo, A. Bhalla (Penn State U.); and U. Balachandran, Quantum Paraelectric-like Behavior of the Paratitanate Family of Materials, *Int. J. Inorganic Mater.* **1** (1999) 395-402.

B. Venkateshwaran, M. Yao, R. Guo, A. Bhalla (Penn State U.), and U. Balachandran, Low Temperature Dielectric Properties of Magnetoplumbite Family of Materials, *Int. J. Inorganic Mater.* **1** (1999) 213-217.

J. R. Hull, Effect of Permanent-magnet Irregularities in Levitation Force Measurements, *Supercond. Sci. Technol.* **13** (2000), 854-856.

B. L. Fisher, K. C. Goretta, N. C. Harris, U. Balachandran; and N. Murayama (Natl. Ind. Res. Inst. of Nagoya), Critical Current Densities in Bi-2223 Sinter Forgings, *Advances in Cryogenic Engineering*, Vol. **46B**, pp. 686-690 (2000), eds. U. Balachandran, D. U. Gubser, K. T. Hartwig, and V. A. Bardos.

J. Martinez-Fernandez, A. Dominguez-Rodriguez (U. de Sevilla); J. L. Routbort and K. C. Goretta, Creep of Polycrystalline  $(\text{Bi,Pb})_2\text{Sr}_2\text{Ca}_2\text{Cu}_3\text{O}_x$ , *Scripta Mater.* **42** (2000) 743-747.

J. L. Routbort, K. C. Goretta, R. E. Cook; and J. Wolfenstine (Army Res. Lab., Adelphi, MD), Deformation of Perovskite Electronic Ceramics: A Review, *Solid State Ion.* **129** (2000) 53-62; invited paper.

J. H. Cheon and J. P. Singh, Cryogenic Deformation and Processing of Ag-Sheathed BSCCO Tapes, Abstract presented at 102nd Annual Meeting of the American Ceramic Society, St. Louis, April 30-May 3, 2000.

D. J. Miller, Z. P. Luo, N. M. Murphy, S. E. Dorris, V. A. Maroni, and H. Claus, Structural Studies of Bulk and Powder-in-Tube Bi-1212 by Transmission Electron Microscopy, Abstract presented at 102nd Annual Meeting of the American Ceramic Society, St. Louis, April 30-May 3, 2000.

B. C. Prorok, J.-H. Park, K. C. Goretta, U. Balachandran; and M. J. McNallan (U. of IL-Chicago), Strengthening of Ag/Bi-2223 Composite Wires by Internal Oxidation of Ag Alloys, Abstract presented at 102nd Annual Meeting of the American Ceramic Society, St. Louis, April 30-May 3, 2000.

T. G. Truchan, M. P. Chudzik, R. A. Erck, K. C. Goretta, and U. Balachandran, Ion-to-Atom Arrival Ratio Dependence of In-Plane Texture in Ytria-Stabilized Zirconia Thin Films, Abstract presented at 102nd Annual Meeting of the American Ceramic Society, St. Louis, April 30-May 3, 2000.

U. Balachandran, Inclined Substrate Deposition (ISD) of MgO for Coated Conductors, Presentation at the European Workshop on Coated Conductors, University of Göttingen, Germany, May 26-27, 2000.

U. Balachandran, MOCVD of YBCO on IBAD Substrates: IGC-ANL-LANL Collaborative Effort, Presentation at the European Workshop on Coated Conductors, University of Göttingen, Germany, May 26-27, 2000.

U. Balachandran, Development of High-Temperature Superconductors for Electric Power Applications, Presentation at State University of Sao Paulo at Ilha Solteira, Brazil, June 14, 2000.

#### Submitted

T. R. Askew (Kalamazoo College) and Y. S. Cha, Transient Response of 50-kA YBCO Rings and Ring Pairs to Pulsed Magnetic Fields, Abstract to be presented at Applied Superconductivity Conf., Virginia Beach, VA, Sept. 17-22, 2000.

U. Balachandran, HTS for Electric Power Applications: Current Status and Future Prospects, Abstract to be presented at THERMEC 2000 – International Conf. on Processing and Manufacturing of Advanced Materials, Las Vegas, Dec. 4-8, 2000.

A. Cansiz (IRC in Superconductivity) and J. R. Hull, Correlation Between Free Oscillation Frequency and Stiffness in HTS Bearings, Abstract submitted to Workshop on Superconducting Flywheels, Eger, Hungary, July 10-11, 2000.

Y. S. Cha and T. R. Askew (Kalamazoo College), Transient Characteristics of a High- $T_c$  Superconductor Tube Subjected to Internal and External Magnetic Fields, Abstract to be presented at Applied Superconductivity Conf., Virginia Beach, VA, Sept. 17-22, 2000.

M. G. Ennis, T. J. Tobin (S&C Electric Co.); J. R. Hull, and Y. S. Cha, Fault Current Limiter - Predominantly Resistive Behavior of a BSCCO Shielded-Core Reactor, Abstract to be presented at Applied Superconductivity Conf., Virginia Beach, VA, Sept. 17-22, 2000.

K. E. Gray, D. J. Miller, M. B. Field, D. H. Kium, and P. Berghuis, Grain-Boundary Dissipation in High- $T_c$  Superconductors, Proc. 6th Intl. Conf. on Materials and Mechanisms of Superconductors and High-Temperature Superconductors, Houston, Feb. 20-25, 2000.

T. M. Mulcahy, J. R. Hull, K. L. Uherka; R. A. Abboud and J. Juna (Commonwealth Res. Corp.), Tests Results of 2-kWh Flywheel Using Passive PM and HTS Bearings, Abstract to be presented at Applied Superconductivity Conf., Virginia Beach, VA, Sept. 17-22, 2000.

#### 1998-2000 Patents

Engineered flux pinning centers in BSCCO, TBCCO and YBCO superconductors  
Kenneth C. Goretta, Michael T. Lanagan, Jieguang Hu, Dean J. Miller, Suvankar Sengupta, John C. Parker, U. Balachandran, Donglu Shi, and Richard W. Siegel  
U.S. Patent 5,929,001 (July 27, 1999).

Method and etchant to join Ag-clad BSCCO superconducting tape  
Uthamalingam Balachandran, A. N. Iyer, and J. Y. Huang  
U.S. Patent 5,882,536 (March 16, 1999).

Elongated Bi-based superconductors made by freeze dried conducting powders  
Uthamalingam Balachandran, Milan Lelovic, and Nicholas G. Eror  
U.S. Patent 5,874,384 (Feb. 23, 1999).

Thin-film seeds for melt processing textured superconductors for practical applications  
Boyd W. Veal, Arvydas Paulikas, Uthamalingam Balachandran, and Wei Zhong  
U.S. Patent 5,869,431 (Feb. 9, 1999).

Superconductor composite  
Stephen E. Dorris, Dominick A. Burlone, and Carol W. Morgan  
U.S. Patent 5,866,515 (Feb. 2, 1999).

Surface texturing of superconductors by controlled oxygen pressure  
Nan Chen, Kenneth C. Goretta, and Stephen E. Dorris  
U.S. Patent 5,856,277 (Jan. 5, 1999).

Method for synthesizing and sinter-forging Bi-Sr-Ca-Cu-O superconducting bars  
Nan Chen, Kenneth C. Goretta, and Michael T. Lanagan  
U.S. Patent 5,821,201 (Oct. 13, 1998).

Mixed-mu superconducting bearings  
John R. Hull and Thomas M. Mulcahy  
U.S. Patent 5,722,303 (March 3, 1998).